NAT. CROAT. | VOL. 35 | No 2 | 0 - 0 | ZAGREB | December 31, 2026

original scientific paper/izvorni znanstveni rad
DOI 10.20302/NC.2026.35.26

PALEOSEISMICITY OF WESTERN TETHYAN EOCENE FORELAND BASIN MARGIN, RAB ISLAND, CROATIA

TIHOMIR MARJANAC*, LJERKA MARJANAC & MARINA ČALOGOVIĆ

Independent researchers, ProGEO-Croatia, Horvatovac 102a, 10000 Zagreb, Croatia

Marjanac, T.; Marjanac, Lj. & Čalogović, M.: Paleoseismicity of Western Tethyan Eocene foreland basin margin, Rab Island, Croatia. Nat. Croat., Vol. 35, No. 2, ______, 2026, Zagreb.

Eocene paralic and incised-valley sediments of eastern Adriatic Rab Island, as a part of western Tethys, comprise 23 horizons of soft- and brittle-sediment deformations interbedded with undeformed shoreface heterolithic sediments and estuarine tidal sandstone bodies. The deformed sediments span in thickness 0.5-8 m, and can be traced for 0.5 km. The soft-sediment deformations include: pseudonodules, flame structures and abiotically homogenized sediments, whereas brittle-sediment deformations consist of sand-injection dykes, small-scale faults and sand wedges The studied succession of Rab Island sandstones documents Eocene paleoseismicity characterized by major seismic events possibly reaching M7 magnitude. Their epicenters were probably located over 100 km from the study area, but some may have been also on Rab Island itself as inferred from synsedimentary kink folds and associated blind thrust faults.

Key words: Paleogene, Dinarides, sedimentary rocks, seismites, liquefaction

Marjanac, T.; Marjanac, Lj. & Čalogović, M.: Paleoseizmičnost ruba eocenskog *foreland* bazena zapadnog Tetisa, otok Rab, Hrvatska. Nat. Croat., Vol. 35, No. 2, ______, 2026, Zagreb.

Eocenski paralički sedimenti i sedimenti usječenih dolina istočnojadranskog otoka Raba, kao dijela zapadnog Tetisa, sadrže 23 horizonta plastično i krto deformiranih sedimenata koji se proslojavaju s nedeformiranim heterolitičnim sedimentima obalnog lica (*shoreface*) i estuarijskim plimnim sedimentnim tijelima. Deformirani sedimenti su debeli od 0,5 do 8 m i mogu se lateralno pratiti oko 0,5 km. Deformirani mekani sedimenti obuhvaćaju: pseudonodule, plamene strukture, i abiotički homogenizirane sedimente, dok deformirani krti sedimenti obuhvaćaju dajkove utisnutog pijeska, male rasjede i pješčane klinove. Istraženi slijed eocenskih pješčenjaka ukazuje na snažne paleoseizmičke događaje moguće magnitude M7. Njihovi epicentri nalazili su se na udaljenosti većoj od 100 km od istraživanog područja, a neki su se mogli nalaziti i na području današnjeg otoka Raba na što ukazuju sinsedimentacijske koljenaste bore i njihovi slijepi reversni rasjedi.

Ključne riječi: paleogen, Dinaridi, sedimentne stijene, seizmiti, likvefakcija

INTRODUCTION

The assessment of seismic hazard is based on data on historical and sub-historical seismicity in a certain region, but seismological catalogues typically miss data on strong earthquakes with long-recurrence time. These may be complemented by data on palaeoearthquakes that have caused specific structures in the rock record. The study of seismically-induced soft-sediment deformation structures can reveal palaeoseismicity that is not

* corresponding author: tihomirmarjanac@gmail.com

recorded in historical or instrumental catalogues, particularly for strong earthquakes with long recurrence intervals. The Rab Island in the northern Adriatic Sea lies geotectonically between the Istrian and Northern Dalmatian flysch basins (Fig. 1). The goal of our research was to achieve better understanding of geological events and sediment deformation processes recorded in the Rab Island Eocene clastic succession. Previous research (MARJANAC & MARJANAC, 2007) documented that the studied sediments were deposited in a shallow paralic sea which was periodically dominated by high-amplitude tides and high-frequency relative sea-level changes. Horizons of deformed sediments were already recognized and interpreted as submarine slumps by MARJANAC & MARJANAC (2007) but have recently been reinterpreted as seismogenic structures (MARJANAC *et al.*, 2022).

Seismically-induced soft-sediment deformation structures, usually referred to as 'seismites' (SEILACHER, 1969) are recognized in many sedimentary basins and comprise deformation structures such as: a) pseudonodules (KUENEN, 1958; OWEN, 2003), b) slumps, c) convolutions, d) flame-structures (DŻUŁYŃSKI & WALTON, 1965; ALLEN, 1984), e) sand volcanoes (LANDUZZI *et al.*, 1995; MONTENAT *et al.*, 2007), and f) sand injections and dykes (OBERMEIER & POND, 1999; MONTENAT *et al.*, 2007), among 120 other features listed by SHANMUGAM (2017). However, many of these features may also be caused by aseismic processes (RICCI LUCCHI, 1995; SHANMUGAM, 2016, 2017) so their attribution to seismic cause is more than ambiguous (MORETTI & VAN LOON, 2014).

In this paper we present the first account of high-magnitude Eocene paleoseismicity of Western Tethyan paralic province of the eastern Adriatic Sea which are complementary to the accounts of other researchers of deep basinal sediments in the Dalmatian depositional basins (e.g. MARJANAC, 1991, 1994). Herein we reinterpret the genesis of soft-sediment deformation structures some of which were previously attributed to slumping (MARJANAC & MARJANAC, 2007), along with newly recognized brittle-sediment deformations.

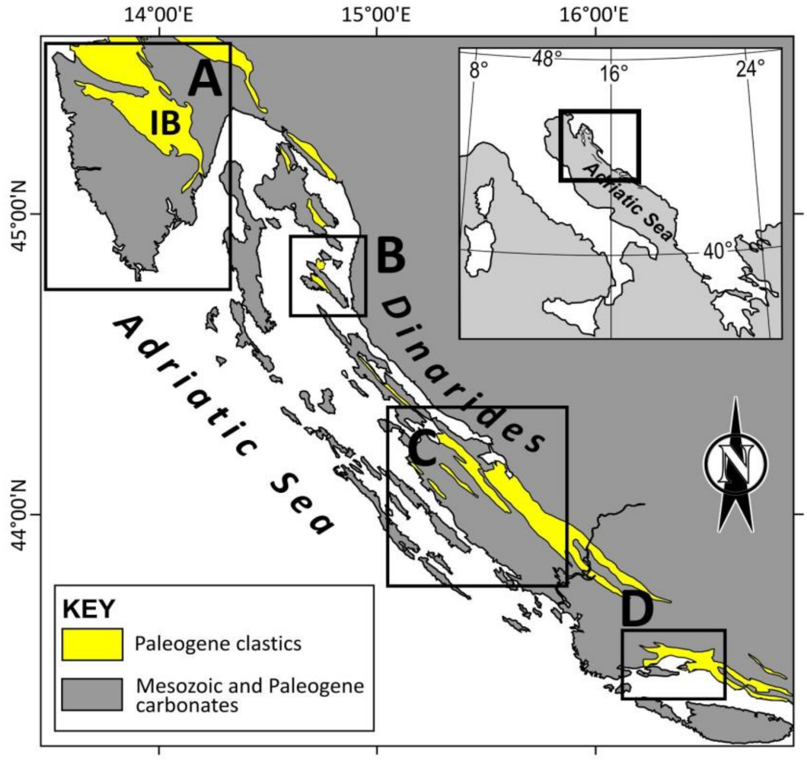

Fig. 1. Position of study areas within Paleogene clastic domains of External Dinarides. (a) IB = Istrian flysch basin; (b) Rab Island basin margin; (c) Northern Dalmatian flysch basin; (d) Central Dalmatian flysch basin. Based on Geological map of SFR Yugoslavia 1:500.000 (Federal Geological Institute, 1970), simplified.

Geology of Rab Island

The oldest exposed deposits on Rab Island are Upper Cretaceous carbonate platform limestones in the cores of two anticlines (MAMUŽIĆ *et al.*, 1969) (Fig. 2). The Cretaceous/Paleogene boundary is marked by a major hiatus and small bauxite pockets. The Paleogene deposits of Rab Island in stratigraphical order comprise lower-middle Eocene Foraminiferal Limestones, Glauconitic marly limestones (usually referred to as "Transitional beds") and middle-late Eocene siliciclastic sediments which are referred to as Lower and Upper Flysch (MAMUŽIĆ, 1962; MAMUŽIĆ *et al.*, 1969; MAMUŽIĆ & MILAN, 1973). However, the 'Lower Flysch' is redefined as lithostratigraphical unit named San Marino Marls (MARJANAC & MARJANAC, 1999, 2004, 2007) – a predominantly marly unit containing only thin sand interbeds (MULDINI-MAMUŽIĆ, 1962), whereas the 'Upper Flysch' is redefined as the Lopar Sandstones that comprise thick sandstones interbedded with marly intervals (MARJANAC & MARJANAC, 1999, 2004, 2007).

The total thickness of the Lopar Sandstones unit exceeds 550 m and comprises 28 complete depositional sequences (MARJANAC & MARJANAC, 1999, 2004, 2007) bounded by well expressed sequence boundaries (Fig. 3).

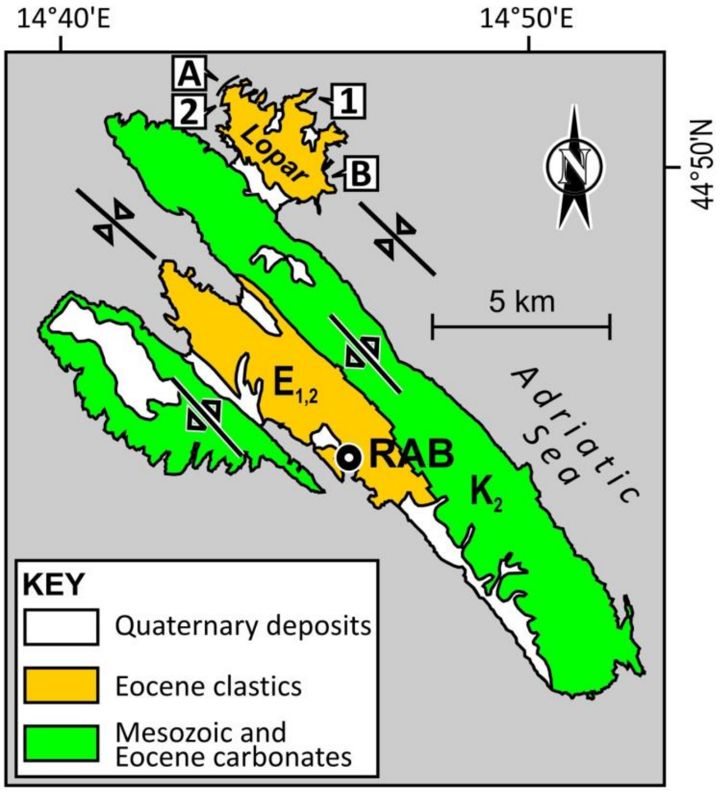

Fig. 2. Geological map of Rab Island after MAMUŽIĆ *et al.* (1969), simplified. Numbers 1 and 2 mark locations of kink folds in Fig. 4. A and B mark locations of sedimentary logs in Fig. 5 and deformed sediments illustrated in Figs. 8 and 9, respectively.

The Lopar Sandstones were deposited in three different environments forming three types of sedimentary bodies: a) lower shoreface thin storm sandstones interbedded with sandy marls, b) middle shoreface sandstone sheets, and c) estuarine tidal sandstone bodies composed of migrating complex sand dunes (MARJANAC & MARJANAC, 2007). The Lopar Sandstones are composed of quartz and chert grains with the provenance outside the present Dinaric range, most likely in the far north European land mass. Their good sphaericity and roundness suggest long-lasting fluvial transport. The Lopar Sandstones unit also comprises several rudite interbeds composed of well-rounded chert and limestone pebbles in addition to abundant skeletal debris of large Eocene shallow-marine bivalves, echinoderms and gastropods that were referred to as the "internal conglomerates" by MARJANAC & MARJANAC (2007). The chert and limestone pebbles most likely originated from the exposed palaeo-Dinaric Mountains, and are the product of weathering of the exposed Mesozoic limestones with diagenetic chert nodules, as interpreted by IVANOVIĆ *et al.* (1978) for the debris in the Eocene Promina Beds of Northern Dalmatia. The skeletal debris, which is mechanically much weaker than the rock pebbles, probably originated from the erosion and redeposition of the coeval shallow marine sediments.

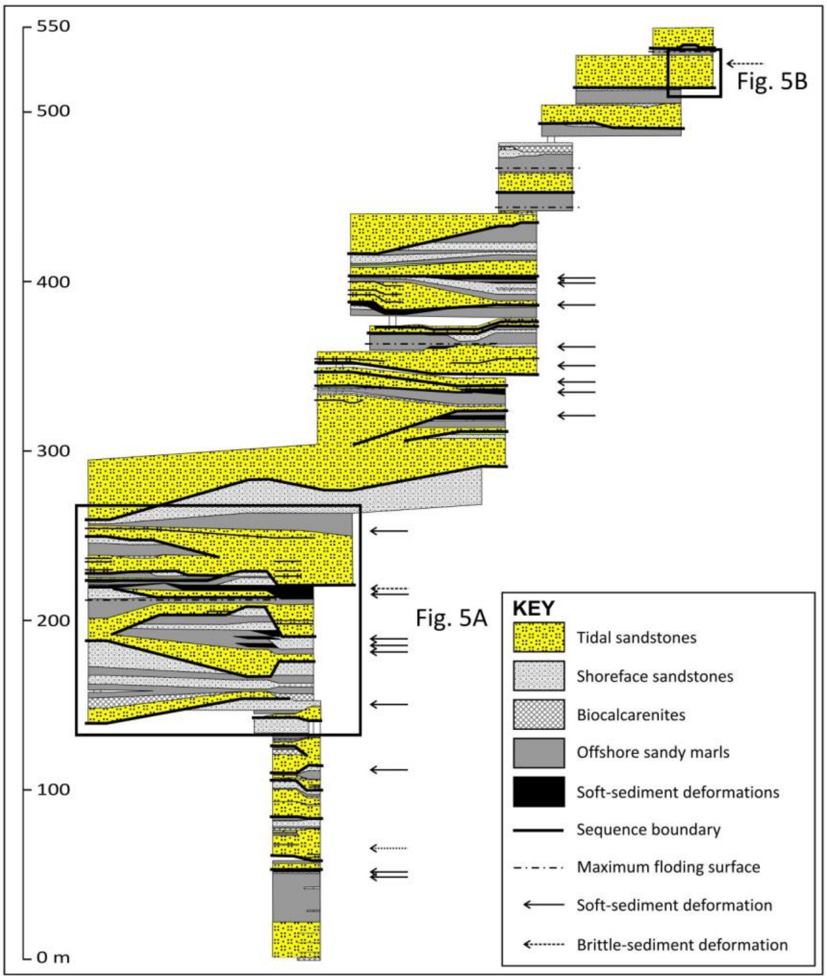

Fig. 3. Simplified composite sedimentary log of Rab Island Eocene Lopar Sandstones unit (MARJANAC & MARJANAC, 2007). Arrows mark horizons of soft- and brittle sediment deformations. Detailed sections are illustrated in Figs. 5A and B.

The sheet sandstones are interpreted as shoreface storm deposits. These are commonly truncated by the bases of overlying cross-bedded sandstone bodies (MARJANAC & MARJANAC, 2007). These shoreface deposits were likely truncated by significant relative sea-level falls and rapid basinward migration of facies, so the bounding unconformities are interpreted as depositional sequence boundaries (Type-1 Sequence boundaries, sensu MITCHUM *et al.*, 1977). The overlying sandstone bodies have internal architecture of sandwaves or complex dunes which were deposited by high-amplitude tidal currents in incised valleys or estuaries (MARJANAC & MARJANAC, 2007) during periods of relative sea-level rise.

The Lopar tidal sandstone bodies are overlain first by thin shell beds composed almost exclusively of nummulite tests, interpreted as storm-beds and referred to as 'biocalcarenites' in Figs. 3 and 4 which are sharply overlain by sandy marls. This sediment succession was deposited as the relative sea-level rise accelerated, and flooded the incised valleys and their interfluves (MARJANAC & MARJANAC, 2007).

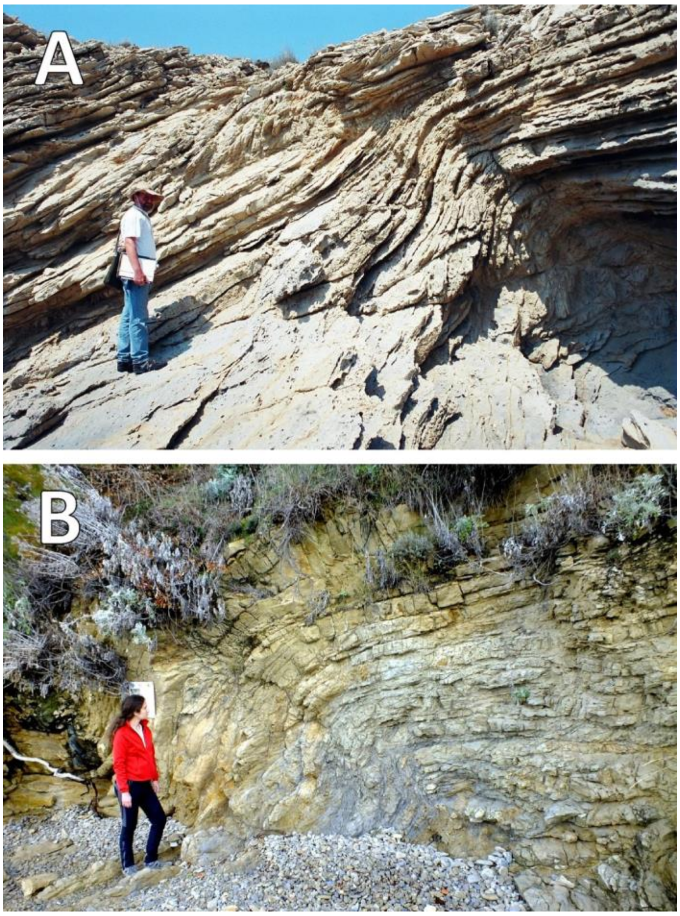

Fig. 4. Kink folds on Lopar Peninsula. (a) Synsedimentary kink fold at 14°45'4.46''E and 44°50'59.95''N (1 in Fig. 2), blind thrust fault is inclined towards NE. The overlying sediments in upper left corner have gentle dip towards SW. (b) Synsedimentary kink fold at 14°43'11.52''E and 44°50'54.25''N (2 in Fig. 2), blind thrust fault is inclined towards SW.

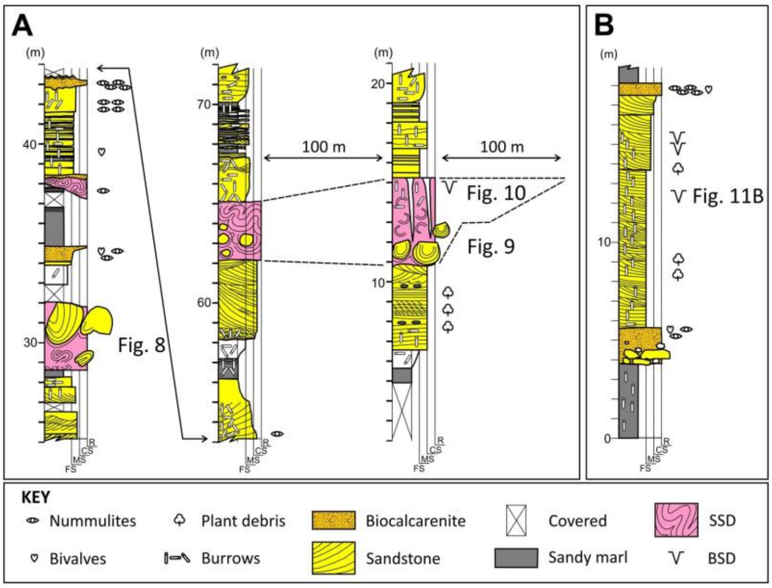

Fig. 5. Detailed sedimentary logs of Lopar Sandstones with marked horizons of soft- and brittle sediment deformations. (a) section with soft-sediment deformations (loc. A in Fig. 2); (b) section with brittle-deformations (loc. B in Fig. 2). Note difference in scale of logs A and B. SSD = soft-sediment deformations, BSD = brittle sediment deformations.

The Lopar sediment succession documents more than 28 episodes of relative sea level rise and fall (MARJANAC & MARJANAC, 2007), which are probably 3rd order sequences *sensu* MITCHUM and VAN WAGONER (1991). Frequent oscillations in relative sea level forced successive basinward and landward shifts of depositional environments. The depositional environments were wave-dominated paralic sea in periods of high sea-level, and tide-dominated incised valley(s) formed during relative sea-level falls and filled during successive relative sea-level rise.

Modern Lopar geological structure is a syncline cut by numerous steep faults with minor slip. However, the Eocene clastic succession of Lopar also hosts two minor synsedimentary kink-folds (Fig. 5).

Age of studied sediments

The Lopar Sandstones are attributed to the middle-late Eocene (MAMUŽIĆ *et al.*, 1969) based on stratigraphic superposition and fossil benthic foraminifera (MULDINI-MAMUŽIĆ, 1962). Dating of Lopar sandstones is so far imprecise due to abundant resedimented foraminifers and nannoplancton (BENIĆ, 1983; MIKES *et al.*, 2008), and absence of planktonic foraminifera. BENIĆ (1983) found nannofossils of the NP16 nannozone (late Lutetian-earliest Bartonian) in the San Marino Marls and noticed predominance of resedimented forms in the Lopar Sandstones, and speculated that they may belong to the same or a younger biozone. MARJANAC & MARJANAC (2007) interpreted the abundance of resedimented macro- and microfossils as a consequence of erosion and resedimentation during periods of relative sea-level falls which caused truncation of the underlying sediments. The sequence stratigraphic study of the Lopar Sandstones (MARJANAC & MARJANAC, 2007) revealed their depositional pattern which was controlled by relative sea-level changes that span from third-order cycle 3.5 to 4.5 of HAQ *et al.* (1987). Herein we consider the Lopar Sandstones to be of late Eocene age based on sequence stratigraphic research and recent discovery of late Eocene - Oligocene palaeomammal Palaeoamassia in the base of one sandstone body (LIHOREAU *et al.*, 2022, 2023).

RESEARCH METHODS

The Rab Island Eocene sandstones were studied by detailed sedimentological logging at a scale of 1:50 (such as in Fig. 4) and facies mapping at a scale of 1:5000. Palaeotransport of sand in sandstone bodies was studied by measuring of dune foresets, where possible. The cumulative thickness of all sedimentary logs is 1191 m, revealing the sediment thickness of over 545 m (Fig. 3). Mineralogical composition of the sandstones was analyzed using standard optical microscopy of stained thin sections, X-Ray diffraction and calcimetry of powdered samples (MARJANAC & ČALOGOVIĆ, 2025).

RESULTS

Detailed sedimentological logging of the Lopar Sandstones revealed 18 horizons of plastically deformed sediments, each exceeding 0.5 m in thickness (Fig. 3), and five horizons displaying brittle sediment deformations.

Plastically deformed sediments

Plastically deformed sediments occur at various stratigraphic levels within the Lopar Sandstones unit. They are sharply but non-erosively bounded by undeformed sediments (MARJANAC & MARJANAC, 2007). Their thickness is over 8 m in the studied sections, although some deformed sediments completely wedge out at a lateral distance of 0.2 km (Fig. 5A).

Three types of plastically deformed sediments were identified, distinguished by the degree of deformation of sandstone beds (Fig. 6) embedded within strongly deformed sandy marl: a) plastically deformed sandstone beds with strongly loaded bases and flat top separated by meter-scale mudstone flame structures (*sensu* DŻUŁYŃSKI & WALTON, 1965) (Figs. 7, 8). These correspond to 'attached pseudonodules' of OWEN (2003), b) convoluted sandstone lumps (Fig. 9) of decimetre- to metre-scale – interpretable as 'pseudonodules' of KUENEN (1958), 'detached pseudonodules' of OWEN (2003), or 'ball-and-pillow' structures of DŻUŁYŃSKI & WALTON (1965) – occurring at several levels within the sandy marl, and c) intensively deformed sandy marls that host deformed sandstones are characterized by convoluted structure ('flow structures' of PLAZIAT *et al*., 1990), with scattered microfossils and locally 'pockets' or lumps of foraminifera. The sediment was probably originally heterolithic, but now looks as intensively bioturbated fluidally-structured sediment. The bluish color indicates deposition in a dysaerobic environment.

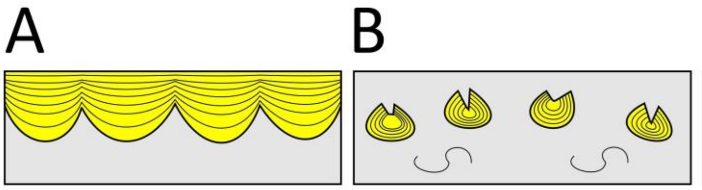

Fig. 6. Plastic sediment deformation. (a) Folded sandstones with strongly loaded lower bedding plane (attached 'pseudonodules') (Fig. 8); (b) Sandstone lumps (detached 'pseudonodules') (Fig. 9). In both cases liquefaction-induced loading of 'pseudonodules' acted into 'homogenized' sandy marls (Fig. 7). Detached 'pseudonodules' may occur at various levels within sandy marl 'matrix', but large ones almost always occur at the marl base (Fig. 10A).

Fig. 7. Plastically deformed sandy marls in the lower part of the section A (Fig. 5A) represent 'matrix' which hosts detached sandstone 'pseudonodules'. Detail, ca. 0.5 m wide. Note intensive folding of originally heterolithic sediment.

Fig. 8. Soft-sediment deformations of Lopar Sandstones, in the lower part of the section A in Fig. 5A. Note large-scale flame structures between attached pseudonodules which is typical for the studied sediments.

Fig. 9. The middle part of the section Fig. 5A. Sandstone lumps are detached pseudonodules which have sunk to the base of soft-sediment deformed bed. Scale is 1 m long measuring stick. The zone of deformed sediment wedges-out at short distance to the right (NW), but is continuous for several hundreds of meters to the left (SE).

The axial planes of folded sandstone lumps ('pseudonodules') and associated flame structures are usually vertical to sub-vertical (Figs. 6A, 7). Compositionally, the plastically deformed sandstones and detached sandstone lumps (Figs. 6B, 8, 9) are identical; the only difference lies in the degree of deformation. The overlying and underlying beds are fully concordant with the surrounding strata and show no signs of synsedimentary deformations, basal erosion or top truncation.

Brittle sediment deformations

Three types of brittle sediment deformations are recognized in the Lopar Sandstones. These structures are generally unrelated to plastically deformed sediments, although both deformation types coincide at one locality. The brittle structures comprise: a) sandstone dykes (Fig. 10), b) small-scale synsedimentary faults (Fig. 11A), and c) sandstone wedges (Fig. 11B).

A) Sandstone dykes (Figs. 5A, 10) are cutting a horizon of plastically deformed sediments with detached 'pseudonodules' (Figs. 5A, 10) extending from the base to the top of the deformed interval, and correspond to the 'intrusion' type dykes of MONTENAT *et al.* (2007). The dykes are vertically oriented, 20 – 40 cm wide and approximately 4 m high, and with lateral spacing of 1 – 2 m. They are filled with vertically laminated sand which is cleaner and coarser-grained (Figs. 10B, C) compared with the sandy marl they cut through. The dyke sandstone is brownish-colored, in contrast to the bluish sandy marl host sediment (Fig. 10B).

B) Small-scale synsedimentary faults (Fig. 11A) occur immediately below the base of a tidal sandstone body. The deformed unit consists of fine-grained laminated sandstone, about 11 cm thick, cut by several reverse faults with throw of several centimetres. The total thickness of deformed sediment is unknown because its top is truncated by the overlying sandstone body.

C) Sandstone wedges are recognized in three horizons within the same tidal sandstone body (Figs. 5B, 11B). They correspond to the 'tixotropic wedges' of MONTENAT *et al.* (2007). The funnel-shaped sandstone wedges are 15 – 37 cm wide and 20 – 35 cm deep, with lateral spacing of 0.9 – 3.3 m. The margins are sharp and some wedges are filled with vertically laminated sandstone indistinguishable from that of the host sandstone body.

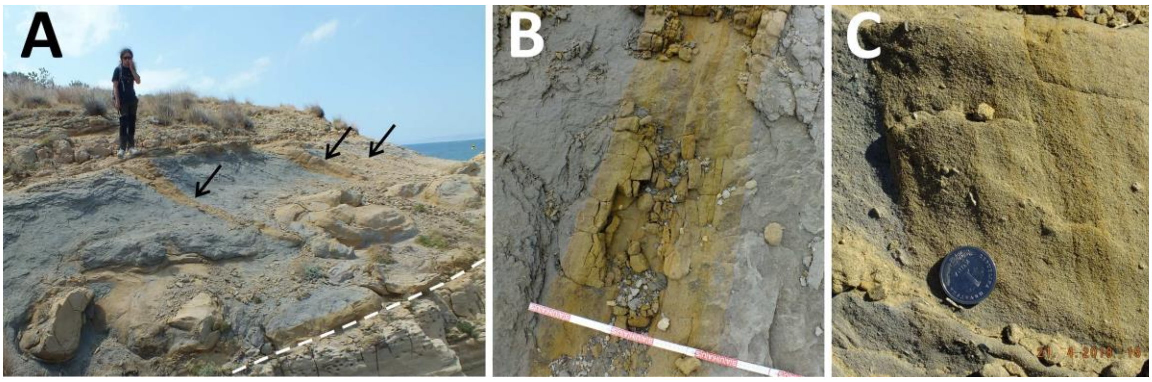

Fig. 10. Brittle sediment deformations superimposed on plastically deformed bed in picture 9 at the distance of ca. 100 m. (A) The base of deformed sediment is marked with a white dashed line. Sandstone dykes are marked by arrows, and they extend from the base to the top of deformed horizon. (B) and (C) Details of sandstone dyke in picture A. The dyke is filled with vertically laminated brownish (oxidized) coarse-grained sandstone which hosts scattered Nummulites, in contrast with bioturbated surrounding bluish sandy marls. Stratigraphic top is upwards, gently tectonically inclined.

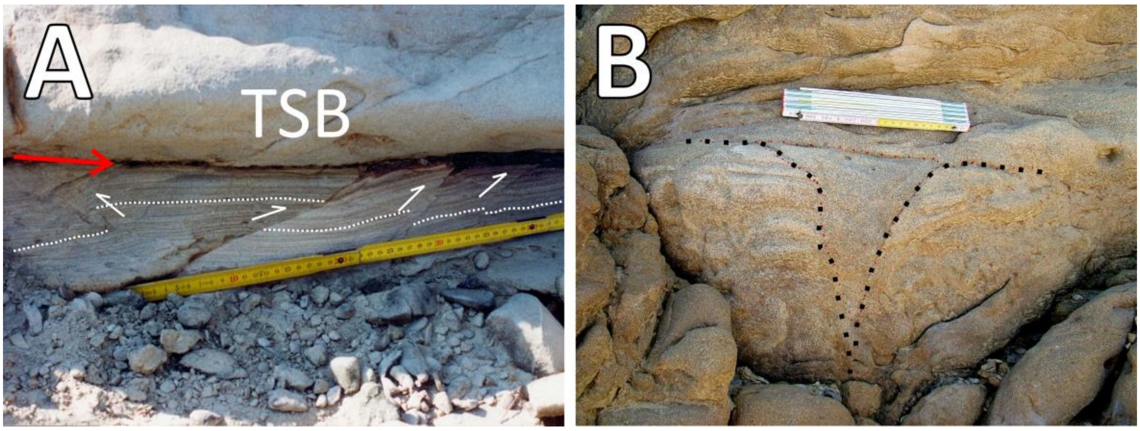

Fig. 11. Brittle sediment deformations. (A) Small-scale faulting in sandstone below a tidal sandstone body not far from the loc. 1 (Fig. 2), note all faults are reverse with throw of several centimetres. Key-bed is dotted white. Basal erosional surface of the tidal body (TSB) is marked by red arrow. (B) Sandstone wedge in tidal sandstones at the section B (Fig. 2, log in Fig. 4B) contoured by dotted black line. Sandstone infill is sometimes laminated parallel to the wedge margins, but compositionally identical to the host sandstone.

DISCUSSION AND INTERPRETATION

Plastically deformed sediments

The Lopar Sandstones were deposited in incised valley systems that were carved by alluvial processes during major relative sea-level falls (MARJANAC & MARJANAC, 2007). Tidal sand bodies were deposited in an incised valley during relative sea-level rise that caused flooding followed by significant increase in tidal range.

The fine-grained offshore (marls, sandy marls) and storm deposits (lower shoreface heterolithics) were deposited in the flooded parts of the incised valley(s) during relative sea-level rise, and on the flooded interfluves during periods of maximal flooding in early highstand. These sand - marl successions show no evidence of small-scale sliding or slumping indicating deposition on essentially horizontal seabed not prone to slope instabilities. It can be argued that the lack of slope instabilities may also indicate a period of tectonic quiescence, with no seismic triggers that would cause slumping, sliding or liquefaction.

Classical rotational slumps and slides typically exhibit sharp, often erosive basal contacts and downslope oriented axial planes. In contrast, the folded sandstone lumps documented here display vertical and sub-vertical axial planes (Fig. 8) implying negligible lateral displacement and dominantly vertical deformation. The associated vertical flame structures further support deformation by liquefaction of unconsolidated sediment, consistent with the experimental results of KUENEN (1958). The absence of basal erosion of the contact with underlying strata indicates that deformation occurred *in situ* through a loss of shear strength of water-saturated sediment.

The sandstones deformation features – both attached (Figs. 6A, 7) and detached (Figs. 6B, 8, 9, 10A) 'pseudonodules' – likely formed through: a) differential and uneven loading of dense sands into a liquefied ("quick") sandy-marl "matrix" (OWEN, 2003), followed by b) vertical expulsion of water-sediment mixtures that produced metre-scale flame structures between individual lumps. The detached sandstone 'pseudonodules' have higher degree of deformation compared to the attached ones, which may be attributed to more intense seismic shaking. The occurrence of both types at separate horizons could indicate differences in earthquake duration(s) or the occurrence of multiple strong aftershocks.

Intense seismic shaking might have also caused intensive liquefaction of the lower shoreface unconsolidated heterolithic sediments that got homogenized with disarticulated remnants of sand layers and fossil beds.

Brittle deformation structures

Brittle deformation structures in the Lopar Sandstones occur in three forms; two of which are generated by a common process; a) clastic dykes and sandstone wedges, and b) small-scale reverse faults. Clastic dykes are recognized cutting sandy marls with 'pseudonodules', sandstone wedges occur within undeformed sandstone bodies, and reverse faults occur in undeformed heterolithic sediments (Fig. 11A).

Clastic dykes were formed through: a) hydrofracturation of low-permeability consolidated and 'homogenized' sandy marls, followed by b) upward intrusion of sand-water slurry from below analogous to the process which generates co-seismic sand volcanoes. The dyke fill is coarser grained than the sand in the surrounding sandy marls, and its vertical lamination indicates upward flow of the liquefied sand-water slurry. Expulsion of water-saturated slurry was probably caused by liquefaction of a sandy aquifer during high-amplitude seismic shaking. The preservation potential of sand volcanoes is very low, and they soon collapse into small craters which are similar to sandstone wedges in the Lopar Sandstones. The collapse of sand volcanoes and infill of craters were observed by the authors during the Petrinja 2020 earthquake.

The occurrence of clastic dykes within the plastically deformed sedimentary package (Figs. 5A, 10A), suggests that both types of structures record a sequence of successive seismic events, likely a major earthquake followed after a short delay by a strong aftershock. The first major seismic event may have caused liquefaction of lower shoreface heterolithic sediments. The second deformation event may have occurred after liquefied sandy marl underwent considerable compaction and reduction of permeability that enabled the sediment to behave in a brittle manner during a later seismic event.

Sand wedges (Fig. 11B) at three stratigraphic levels within the same tidal sandstone body were probably formed by shear stress during three separate syn-depositional seismic events. The shear stress caused hydrofracturation of sand and formation of open cracks which were conduits for expulsion of water-sand slurry. This process likely formed small sand volcanoes that rapidly collapsed into funnel-shaped craters, soon after the expulsion ended. The resulting wedges are filled partly with sand which was intruded from below, but also with sand collapsed from the depositional surface during crater formation.

The small-scale reverse faulting confined to one deformed sandstone layer (Fig. 11A) may have been caused by a compressional seismic wave which affected consolidated sediments, forming a set of centimetre-scale thrust faults. The original thickness of this faulted sediment is unknown because it is truncated by the erosional base of the overlying tidal sand wave.

Palaeoseismicity

Attribution of all soft-sediment deformation structures to seismic origin is controversial as the same features may also be formed by spontaneous liquefaction or loading of rapidly deposited water-saturated sediment, as common in turbidites (LOWE, 1976). Large-scale hydroplastic deformations are widely regarded as the most reliable indicator for seismites (SEILACHER, 1984), so we have restricted seismogenic interpretation only to structures over 0.5 m in thickness, as well as brittle deformation structures that are usually attributed to seismogenic origin regardless of their size (OBERMEIER & POND, 1999). Based on these criteria, the Lopar Sandstones preserve evidence for approximately 23 strong seismic events recorded in the Eocene succession of the Rab Island.

Active basin-forming tectonics appears to be the most plausible driver of the inferred seismicity, as the Late Eocene was a period during which several flysch basins in this part of the Tethys were widening (MARJANAC, 1991; MARJANAC & ĆOSOVIĆ, 2000; ĆOSOVIĆ *et al.*, 2008). The distance of these basins from the Rab Island is approximately 70 km (Istrian Basin), 100 km (Northern Dalmatian Basin), and 190 km (Central Dalmatian Basin) (Fig. 1).

The magnitude of palaeoearthquakes cannot be directly determined, so various approaches have been developed to tackle this problem (see OBERMEIER & POND, 1999). One of the methods involves correlating geomechanical effects like liquefaction with historical earthquakes of known macroseismic intensity (MCS, MMI). In a subsequent step, the deformation features are related to peak-ground acceleration (PGA). Many authors have adopted earthquake intensity as an actualistic analogue in studies of earthquake-induced soft-sediment deformation, including structures of prehistoric age, to attribute the deformation features to a possible earthquake magnitude (eg. OBERMEIER & POND, 1999; GALLI, 2000; MORETTI, 2000).

Liquefaction is commonly triggered by strong earthquakes with the MCS intensity of 5.5° – 11° (GALLI, 2000). SIMS (1973) studied sub-recent and recent deformation structures in a drained artificial lake, which were attributed to historical earthquakes of M5.2 to M7.7 and speculated that generation of pseudonodules may require strong earthquakes with sufficient energy released and long shaking duration. Large-magnitude earthquakes may trigger liquefaction at epicentral distances of hundreds to thousands of kilometers (MUNSON *et al.*, 1995; GALLI, 2000). Following Eq. 14 in GALLI (2000) and PAPATHANASSIOU *et al.* (2005) M7 earthquakes may cause liquefactions at epicentral distance of 130 km, whereas for the M8 earthquake it may occur at the distance of 420 km, although these values may differ from one region to another due to different properties of the local substrate.

Two Rab Island kink folds (Fig. 4) were created by blind thrust faults dipping towards SW and NE, respectively. Such faults are usually considered seismogenic, so these Late Eocene synsedimentary faults may have also generated strong earthquakes. If so, these may have caused some of the observed deformation features, in which case the seismic source was local. If the 4 m thick plastically deformed sandstone unit was completely liquefied the peak ground acceleration estimated using Ishikara's method (OBERMEIER & POND, 1999) would have been approximately 0.25 g. Such acceleration corresponds to the Modified MCS Intensity of 8°-9° that is typically caused by an M7 magnitude earthquake.

CONCLUSIONS

Liquefaction caused near-complete homogenization of lower shoreface heterolithic sediments into sandy marls, locally displaying convoluted and fluidal structures. It was followed by local dewatering and fluidization as documented by large-scale flame structures, sand injections and water-escape pipes which locally cross-cut previously liquefied sediment.

Large-scale pseudonodules and homogenized sandy marls are interpreted as the products of liquefaction because they occur at random stratigraphic positions in the Eocene sedimentary succession unrelated to depositional facies, have vertical axis-planes of folded pseudonodules and sub-vertical flame structures.

Liquefaction and hydrofracturation were most likely triggered by high-acceleration and high-magnitude earthquakes which were followed by a series of high-acceleration aftershocks. Strong aftershocks or the following strong earthquakes may have induced additional liquefaction and fluidization of already weakened sediment, as well as hydrofracturation that facilitated upward sand injections from below. The earthquake acceleration of 0.25 g was estimated after dimensions of clastic dykes, which is in the literature reported to correlate with the MCS intensity of 8°/9° and M7 magnitude.

Large-scale plastically deformed sediments in the Lopar sandstones are therefore interpreted as seismically induced liquefaction products which document strong seismicity that affected unconsolidated paralic sediments at the Eocene basin margin of the Western Tethys.

Brittle sediment deformations are commonly interpreted as seismically induced fracturation features that formed in consolidated sediments, some of which were infilled with intruded sediments from below, or by slumping of sand from steep crater margins, in a process which forms modern co-seismic sand volcanoes.

ACKNOWLEDGMENTS

We are indebted to our former student A. M. Tomša for her help and enthusiasm during the field research. Our ideas were shaped by discussions in the field with many colleagues over the years of research, S. Leszczynski, W. Nemec and M. Poljak in particular. The authors are also indebted to three anonymous reviewers whose comments were very helpful and greatly improved the manuscript. This research was partly funded by the Ministry of Science, Education and Sport of The Republic of Croatia through research projects 1-09-084, 119303 and 119-0000000-1164, and partly by Rab Geopark project of the Municipality of Rab, all lead by T. M. and there is no conflict of interest. The research projects were administrated by the University of Zagreb, and there are no permissions for publication needed.

Received January 29, 2025

REFERENCES

ALLEN, J.R.L., 1984: Sedimentary structures, their characteristics and physical basis. 2nd edn. Developments in sedimentology, 30, XXVI+663, Elsevier, Amsterdam.

BENIĆ, J., 1983: Vapnenački nanoplankton i njegova primjena u biostratigrafiji krednih i paleogenskih naslaga Hrvatske. Doctoral Thesis. University of Zagreb, 159 pp.

ĆOSOVIĆ, V., MARJANAC, T., DROBNE, K. & MORO, A., 2008: Outer Dinarides: eastern Adriatic coast. In: MCCANN, T. (ed.), Geology of Central Europe, 2., 76–80, Geological Society of London, London, U.K.

DŻUŁYŃSKI, S. & WALTON, K., 1965: Sedimentary features of flysch and greywackes. Developments in sedimentology, 7, VI+274, Elsevier, Amsterdam.

FEDERAL GEOLOGICAL INSTITUTE, 1970: Geological Map of SFR Yugoslavia 1:500.000. Institute for geological and mining exploration and investigation of nuclear and other mineral raw minerals. Beograd.

GALLI, P., 2000: New empirical relationships between magnitude and distance for liquefaction. Tectonophysics, 324, 169–187.

HAQ, B.U., HARDEBOL, J. & VAIL, P.R, 1987: Chronology of Fluctuating Sea Levels Since the Triassic. Science, 235, 1156–1166.

IVANOVIĆ, A., SIKIRICA, V. & SAKAČ, K. 1978: Osnovna geološka karta SFRJ 1:100000., Tumač za List Drniš, K 33-9, 5-59, Institut za geološka istraživanja, Zagreb, Savezni geološki zavod Beograd.

KUENEN, Ph.H., 1958: Experiments in Geology. Trans. Geol. Soc. Glasgow, 23, 1–35, Geological Society of Glasgow, Glasgow.

LANDUZZI, A., NICHOLS, R. & VAI, G.B., 1995: Sand Volcanoes in the Marnoso-Arenacea Formation (Miocene, Northern Apennines, Italy): New Evidence of Paleoseismicity. In: SERVA, L. & SLEMMONS, D.B. (eds.), Perspectives in Paleoseismology. Association of Engineering Geologists Special Publication, 6, 49–61, Association of Engineering Geologists. Washington DC., U.S.A.

LIHOREAU, F., MARJANAC, L., MARJANAC, T., ERDAL, O. & ANTOINE, P.-O., 2022: New remains of palaeoamasiine embrithopod (Mammalia, Afrotheria) from the Adriatic realm (Lopar, Island of Rab, Croatia). Abstracts 1st International multidisciplinary symposium Geopark & Sciences - From research to Geotourism. 6-9 October 2022, Rab, Croatia. 49.

LIHOREAU, F., MARJANAC, L., MARJANAC, T., ERDAL, O. & ANTOINE, P.-O., 2023: A Late Eocene palaeoamasiine embrithopod (Mammalia, Afrotheria) from the Adriatic realm (Island of Rab, Croatia). Palaeovertebrata, **47**, 1–11.

LOWE, D.R., 1976: Subaqueous liquefied and fluidized sediment flows and their deposits. Sedimentology, 23, 285–308.

MAMUŽIĆ, P., 1962: Novija geološka istraživanja otoka Raba. Geološki vjesnik, **15**/1, 121–141.

MAMUŽIĆ, P. & MILAN, A., 1973: Osnovna geološka karta SFRJ 1:100.000, Tumač za list Rab L33-144, 5–39, Institut za geološka istraživanja Zagreb, Savezni geološki zavod, Beograd.

MAMUŽIĆ, P., MILAN, A., KOROLIJA, B., BOROVIĆ, I. & MAJCEN, Ž., 1969: Basic Geological Map of SFRY 1:100.000, Sheet Rab, L 33-114, Institute for geological exploration Zagreb, Federal Geological institute, Beograd.

MARJANAC, T., 1991: Importance of megabeds for reconstruction of Paleogene flysch basin in Split hinterland (Middle Dalmatia). Geološki vjesnik, 44, 201–213.

MARJANAC, T., 1994: Evolution of Eocene-Miocene flysch basin of Central Dalmatia, Croatia. Doctoral Thesis, Faculty of Science, University of Zagreb. 348 pp.

MARJANAC, T. & ČALOGOVIĆ, M., 2025: Weathering rate of Late Eocene clastics of Lopar Peninsula (Rab Island, Croatia). Natura Croatica, **34**(1), 37–51.

MARJANAC, T. & ĆOSOVIĆ, V., 2000: Tertiary Depositional History of Eastern Adriatic Realm. In: PAMIĆ, J. & TOMLJENOVIĆ, B. (eds.), Outline of the geology of the Dinarides and south Tisia with field guidebook. Vijesti Hrv. geol. društva, **37**, 93–103.

MARJANAC, T. & MARJANAC, LJ., 1999: Eocene clastics of the Rab island - Lopar peninsula, Rab. In: Some Carbonate and Clastic Successions of the External Dinarides. Field-trip guidebook, Harold Reading's I.A.S. Lecture Tour '99, pp. 29–51, Hrv. geol. društvo, Zagreb.

MARJANAC, T. & MARJANAC, LJ., 2004: Stop 2.1: Eocene incised valley fill clastics of the island of Rab. Adriatic-Dinaric Mesozoic carbonate platform, environments and facies from Permian to recent time. Field-trip guidebook - P53, 32nd International Geological Congress, Florence 2004, Italy., 16–21.

MARJANAC, T. & MARJANAC, LJ., 2007: Sequence stratigraphy of Eocene incised valley clastics and associated sediments, Island of Rab, Northern Adriatic Sea, Croatia. Facies, **53**, 493–508.

MARJANAC, T., MARJANAC, LJ. & ČALOGOVIĆ, M., 2022: Study of Late Eocene seismicity in Lopar Sandstones of Rab Island, Croatia. Abstracts 1st International multidisciplinary symposium Geopark & Sciences - From research to Geotourism. 6-9 October 2022, Rab, Croatia, 36–39.

MIKES, T., BÁLDI-BEKE, M., KÁZMÉR, M., DUNKL, I. & VON EYNATTEN, H., 2008: Calcareous nannofossil age constraints on Miocene flysch sedimentation in the Outer Dinarides (Slovenia, Croatia, Bosnia-

Herzegovina and Montenegro). In: SIEGESMUND, S., FÜGENSCHUH, B. & FROITZHEIM, N. (eds.), Tectonic Aspects of the Alpine-Dinaride-Carpathian System. Special Publications, 298, 335–363. Geological Society, London.

MITCHUM, R.M.JR. & VAN WAGONER, J.C., 1991: High-frequency sequences and their stacking patterns: sequence-stratigraphic evidence of high-frequency eustatic cycles. Sedimentary Geology, **70**, 131–160.

MITCHUM, R.M.Jr., VAIL, P, THOMPSON, III S., 1977: Seismic Stratigraphy and Global Changes of Sea Level, Part 2: The Depositional Sequence as a Basic Unit for Stratigraphical Analysis. In: PAYTON, C.E. (ed.), Seismic Stratigraphy - applications to hydrocarbon exploration. AAPG Mem., **26**, 53–62.

MONTENAT, CH., BARRIER, P., D'ESTEVOU, PH.O. & HIBSCH, CH., 2007: Seismites: An attempt at critical analysis and classification. Sedimentary Geology, 196, 5–30.

MORETTI, M., 2000: Soft-sediment deformation structures interpreted as seismites in middle-late Pleistocene aeolian deposits (Apulian foreland, southern Italy). Sedimentary Geology, 135, 167-179.

MORETTI, M. & VAN LOON, A.J., 2014: Restrictions to the application of >diagnostic= criteria for recognizing ancient seismites. J. Palaeogeogr., **3**, 162–173.

MULDINI-MAMUŽIĆ, S., 1962: Mikrofaunističko istraživanje eocenskog fliša otoka Raba. Geološki vjesnik, **15**(1), 143–159.

MUNSON, P.J., MUNSON, C.A. & POND, E.C., 1995: Paleoliquefaction evidence for a strong Holocene earthquake in south-central Indiana. Geology, **23**, 325–328.

OBERMEIER, S.F. & POND, E.C., 1999: Issues in Using Liquefaction Features for Paleoseismic Analysis. Seismol. Res. Lett., **70**, 34–58.

OWEN, G., 2003: Load structures: gravity-driven sediment mobilization in the shallow subsurface. In: VAN RESENBERGEN, P., HILLS, R.R., MALTMAN, A.J. & MORLEY, C.K. (eds.), Subsurface Sediment Mobilization. Geol. Soc. London Sp. Publ., 216, pp. 21–34.

PAPATHANASSIOU, G., PAVLIDES, S., CHRISTARAS, B. & PITILAKIS, K., 2005: Liquefaction case histories and empirical relations of earthquake magnitude versus distance from broader Aegean region. J. Geodyn., 40, 257–278.

PLAZIAT, J.-C., PURSER, B. & PHILOBBOS, E., 1990: Seismic deformation structures (seismites) in the syn-rift sediments of the NW Red Sea (Egypt). Bull. Soc. géol. Fr., ser. 8, *6*, 419–434.

RICCI LUCCHI, F., 1995: Sedimentological Indicators of Paleoseismicity. In: SERVA, L. & SLEMMONS, D.B. (eds.), Perspectives in Paleoseismology. Association of Engineering Geologists Special Publication, 6, Association of Engineering Geologists, Washington, DC, U.S.A, pp. 7–17.

SEILACHER, A., 1969: Fault-graded beds interpreted as seismites. Sedimentology, **13**, 155–159.

SEILACHER, A., 1984: Sedimentary structures tentatively attributed to seismic events. Mar. Geol., **55**, 1–12.

SHANMUGAM, G., 2016: The seismite problem. J. Palaeogeogr., **5**, 318–362.

SHANMUGAM, G., 2017: Global case studies of soft-sediment deformation structures (SSDS): Definitions, classifications, advances, origins, and problems. J. Palaeogeogr., **6**, 251–320.

SIMS, J.D., 1973: Earthquake-Induced Structures in Sediments of Van Norman Lake, San Fernando, California. Science, **182**, 161–163.